Energy storage and polarization switching kinetics of (001)-oriented $Pb_{0.97}La_{0.02}(Zr_{0.95}Ti_{0.05})O_3$ antiferroelectric thick films

C. Liu,[1] S. X. Lin,[1] M. H. Qin,[1] X. B. Lu,[1] X. S. Gao,[1] M. Zeng,[1,a)] Q. L. Li,[3] and J.-M. Liu[1,2,b)]
[1]*Institute for Advanced Materials and Laboratory of Quantum Engineering and Quantum Materials, South China Normal University, Guangzhou 510006, China*
[2]*Laboratory of Solid State Microstructures and Innovative Center for Advanced Microstructure, Nanjing University, Nanjing 210093, China*
[3]*Department of Electrical and Computer Engineering, George Mason University, Fairfax, Virginia 22033, USA*

(Received 21 February 2016; accepted 10 March 2016; published online 17 March 2016)

For antiferroelectric (AFE) energy storage, the stability of energy storage density and conversion efficiency against wide temperature (T) range and broad frequency (f) band is highly preferred. In this work, we investigate the energy storage and associated kinetics of polarization switching in (001)-textured AFE $Pb_{0.97}La_{0.02}(Zr_{0.95}Ti_{0.05})O_3$ (PLZT 2/95/5) thick films prepared by sol-gel method. A recoverable energy storage density (W_{re}) of ~26.8 J/cm^3 and an energy conversion efficiency (η) as high as ~62.5% have been obtained under an electric field of 1.85 MV/cm and room temperature. Both the W_{re} and η are only weakly T-dependent up to 280 °C and weakly f-dependent ranging from 20 Hz to 10 kHz. The high frequency stability originates from the rapid polarization switching as identified by the nucleation-limited-switching theory, suggesting a characteristic switching time as short as ~3 ns, favorable for applications in pulse energy storage. © *2016 AIP Publishing LLC*. [http://dx.doi.org/10.1063/1.4944645]

Dielectric materials exhibiting high energy-storage density and fast charge-release have been extensively studied for their potential applications in power electronic systems.[1–3] For a dielectric, the energy storage density per unit volume, W, can be estimated from the polarization (P) vs. electric field (E) hysteresis, expressed by $W = \int E \cdot dP$.[4] Given increasing E from zero to the maximum field (E_m), polarization P is enhanced up to the maximal P_m, and the stored energy storage density is denoted as W_{st}. The recoverable energy storage density denoted as W_{re} is then released upon discharging from E_m to zero. The energy conversion efficiency (η) is defined as $\eta = W_{re}/W_{st}$.

Based on this definition, it is expected that linear dielectrics or paraelectrics (PE) exhibit a high η because of the slim hysteresis loops or low energy loss,[5] while they usually have low W due to the low P_m. Ferroelectrics (FE) process a high P_m, but also a high remanent polarization (P_r) contributing to large energy loss.[6] Comparably, antiferroelectric (AFE) materials, exhibiting large P_m and nearly zero P_r (i.e., slim hysteresis loops), are considered as effective dielectrics for high energy storage capacitors.[4,7] Lead lanthanum zirconate titanate [$Pb_{1-x}La_x(Zr_yTi_z)O_3$, PLZT $x/y/z$, usually with $z = 1 - y$ and $x/y/z$ scaled in percentage]-based materials represent one of the most promising candidates for high energy storage capacitors.

Currently, quite a number of investigations on PLZT-based AFEs for energy storage performance have been reported.[4,7–22] For examples, a $W_{re} \sim 0.698$ J/cm^3 was realized in PLZT-based AFE ceramics,[8] while a W_{re} as high as ~85 J/cm^3 in PLZT thick films was reported by Ma *et al.*[7] Also, Hu *et al.*[14] revealed a high W_{re} of ~61 J/cm^3 along with a low η of ~33% for PLZT 4/98/2 thin films. Generally, the bulk PLZT-based ceramics usually have low W_{re} due to the low E_m limited by the materials quality (porosity).[15] The improved W_{re} is usually achieved in thin film form at the cost of substantial decrease of energy storage quantity. Compromises have thus been made by adopting thick films (>1 μm) as effective structures to overcome these disadvantages in thin films and bulk ceramics.

For practical applications, high thermal stability, i.e., robustness of the energy storage density against varying temperature (T) is preferred.[3,14,17–20] For instance, good thermal stability in PLZT 2/98/2 thick films[17] and $Pb_{0.97}La_{0.02}(Zr_{0.58}Sn_{0.035}Ti_{0.085})O_3$ ceramics[19] were reported. On the other hand, high stability of the energy storage (density and efficiency) over a broad range of frequency (f) (or inverse periodicity) of electric field (E) is also required. Earlier investigations revealed that the frequency dependence is also weak for most AFE films.[17,18] Fundamentally, the dielectric energy storage in AFE materials must be essentially related to the details of polarization switching driven by field E. In fact, it has been demonstrated that the energy discharge efficiency of a power capacitor is significantly influenced by the field frequency.[2] Nevertheless, the polarization switching in an AFE system is far from understood, different from the case of an FE material where the dynamic hysteresis has been well investigated.[6,23–26]

Along this line, it would be of great importance to investigate the kinetics of polarization switching for AFE thick films in order to understand the high thermal and frequency stability of the energy storage performances (W_{re} and η), which has unfortunately not yet established. In this work, we first prepared highly (001)-textured PLZT 2/95/5 thick films on Pt-coated Si substrates. Then, under stimulation of an electric field E, the energy storage density W_{re} and efficiency

a)E-mail: zengmin@scnu.edu.cn
b)E-mail: liujm@nju.edu.cn

η of the thick films as a function of T and f, with $T \in (25\,^{\circ}\text{C}, 280\,^{\circ}\text{C})$ and $f \in (2.0\,\text{Hz}, 10\,\text{kHz})$, were measured. By means of the nucleation-limited-switching (NLS) theory, the polarization switching kinetics is discussed, predicting that the characteristic time for the polarization switching can be as short as $\sim$3 ns. The present work thus provides a basis for understanding the high stability of the energy storage performances against varying T and f for the PLZT 2/95/5 thick films.

The PLZT 2/95/5 thick films prepared on commercially available Pt(111)/Ti/SiO_2/Si(100) (Pt/Si) substrates using the conventional sol-gel method.[22] The details of the solution preparation and deposition conditions can be found in the supplementary materials.[29] For measuring the ferroelectric properties, the top Pt electrodes with 200 μm in diameter were deposited through transmission electron microscopy grids by pulse laser deposition. The *P-E* hysteresis loops were measured using the Precision Multiferroic tester (Radiant Technologies, Inc.) in the normal virtual-ground mode, and the polarization switching kinetics was investigated under the positive up negative down (PUND) mode. The *T*-dependent measurements were performed in a sample stage set-up in the closed heating furnace with good thermal stability. Given the sufficient *P-E* loop data over broad ranges of T and f, one is allowed to evaluate the energy storage density and efficiency as well as the dependences of W_{re} and η on T and f, respectively.

In this work, the PLZT 2/95/5 thick films were well crystallized into polycrystalline perovskite phase with highly (001)-texture, see supplementary material Fig. S1[29] as an example. The film surface is dense and void-free and its thickness is $\sim$1.2 μm with dense and column-like grains (supplementary materials, Fig. S2[29]). First, the thermal stability of the energy storage property in our thick films is characterized by the *P-E* loops measured at $T = 25\,^{\circ}\text{C}$ to $280\,^{\circ}\text{C}$ with $f = 1.0$ kHz. Fig. 1(a) presents the *P-E* loops measured at four different T under 1.25 MV/cm, revealing the significant impact of T on the hysteresis shape. The double-loop hysteresis evolves gradually into slim single-loop hysteresis, attributing to the AFE $\rightarrow$ FE phase transition, similar to earlier results.[17,19,20] What should be mentioned here is that either W_{re} or η does not necessarily fall with increasing T, considering the details of the loop shape evolution. While a larger P_r at higher T is observed, the hysteresis becomes more inclined, implying possibly enhanced W_{re} or η with increasing T. The evaluated $W_{re}(T)$ and $\eta(T)$ curves at three different E are shown in Fig. 1(b). It is seen that the η does gradually grow first and decays then with increasing T, consistent with the above argument. The highest η can be above 80% at $T \sim 180\,^{\circ}\text{C}$ at proper E (i.e., $\sim$1.0 MV/cm). The W_{re} under very high E also shows slight enhancement with increasing T, while it may fall slightly at low E. Nevertheless, in the overall tendency, the T-dependences of both W_{re} and η are weak, implying that both W_{re} and η have quite good thermal stability. Surely, as T approaches 280 °C, the electrical leakage becomes too big and a reliable measurement under high electric field becomes difficult.[14] It should be noted that the evaluated W_{re} or η depends remarkably also on the electric field, as shown by several typical

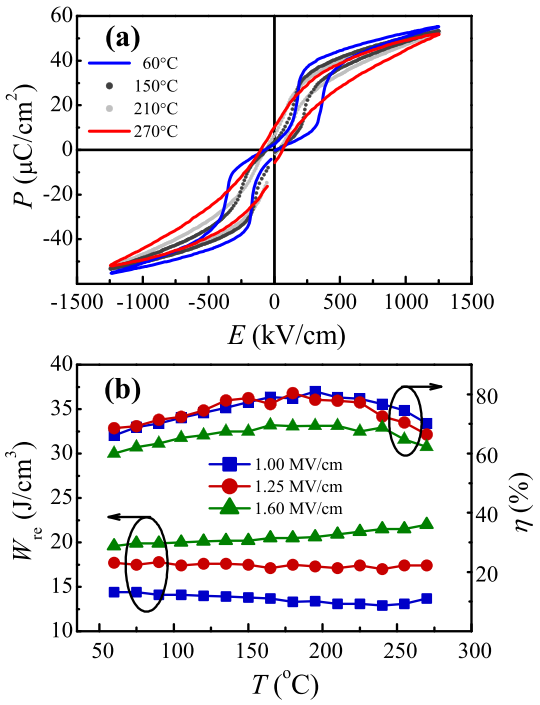

FIG. 1. (a) Selected P-E hysteresis loops at different T with a given electric field E of 1.25 MV/cm. (b) T-dependent energy storage density (W_{re}) and efficiency (η) at three different electric fields for the PLZT 2/95/5 thick films.

loops measured under different E, and evaluated $W_{re}(E)$ or $\eta(E)$ dependence in supplementary materials, Fig. S3.[29]

Next, we look at the dynamic hysteresis for the PLZT 2/95/5 thick films over $f \in (2.0\,\text{Hz}, 10\,\text{kHz})$ at room temperature, given $E \sim 0.6$ MV/cm ($> E_F \sim 0.35$ MV/cm, here E_F is the field-induced forward AFE $\rightarrow$ FE switching field). The data at four frequencies are shown in Fig. 2(a). Obviously,

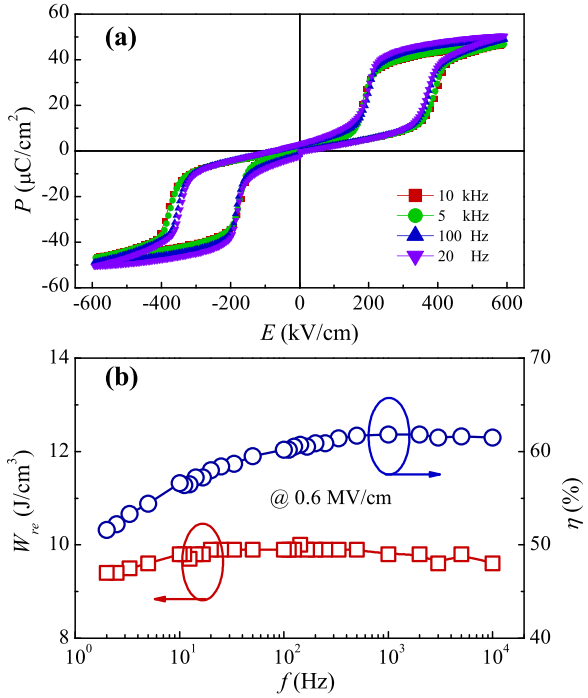

FIG. 2. (a) Selected P-E hysteresis loops at different frequencies (f) with a given electric field of 0.6 MV/cm, and (b) frequency-dependent energy storage density (W_{re}) and efficiency (η) of the PLZT 2/95/5 thick films.

the f-dependence is not very significant, although a tiny change of the hysteresis shape would have visible impact on W_{re} and η. Consequently, the evaluated $W_{re}(f)$ and $\eta(f)$ curves are depicted in Fig. 2(b). One observes a variation of η for ~20% and a variation of W_{re} for ~5% with the f variation over $f \in (2.0\,\text{Hz}, 10\,\text{kHz})$. The data measured at other temperatures show similar behaviors unless $T > 280\,^{\circ}\text{C}$. It is thus revealed that the PLZT 2/95/5 thick films exhibit high frequency stability in the energy storage properties.

One may argue that the ultra-fast polarization switching of an AFE system is the core origin for such high frequency stability. We consult to the kinetics of polarization switching driven by field E of different f under room temperature. This kinetics, similar to the case of a FE system, may be described by the NLS theory.[23–26] Here, the switching polarization P as a function of time t can be expressed as[25]

$$P(t) = \int_{-\infty}^{\infty} \{1 - \exp[-(t/t_0)^n]\} F(\log t_0) d(\log t_0), \quad (1)$$

where t_0 is the waiting time of the elementary domain regions, i.e., the characteristic time for polarization switching, n is the effective dimension, and $F(\log t_0)$ is the Lorenzian distribution function for $\log t_0$.

To fit the measured data by the NLS model, we adopted the PUND method to measure the switching polarization (P_{sw}) and nonswitching polarization (P_{ns}). The schematic is shown in supplementary materials, Fig. S4.[29] It is convenient to discuss the measurent P_{sw} with the theroical polarization in the NLS model by defining the normalized P_{sw} as P_{nz}. Fig. 3 dispicts P_{nz} (symbols) as a function of t under various E, and the numbers are the field magnitudes. It is noted that the switching was almost completed in less than 7.0 μs when the pulse magnitude was increased up to ~500 kV/cm.

Based on the above $P(t, E)$ data, one adopts the NLS model to evaluate the polarization switching time for the present thick films. The NLS model describes the domain nucleation as a region-by-region dominated process, with each elementray region containing a limited number of nucleation centers. The definition of the volume fraction of polarization can be given by

$$p(t) = 1 - \sum_{ns} S_i \Big/ \sum_{all} S_i, \quad (2)$$

where bottom subscript ns means the nonswitched volume by time t. By introducing a Lorenzian distribution function for local swiching times ($g(z)$) and neglecting with the logarithmic accuracy, the correleation between the distribution of typical waiting time τ_i for elementary region I, and the ratio γ_i for the area of region i, we can obtain the following expression for $p(t)$:

$$p(t) = \begin{cases} \Gamma h\left(\frac{\pi}{2} - \arctan\left(\frac{z_1 - z_0}{\Gamma}\right)\right), & z_0 < z_1 \\ \Gamma h\left(\frac{\pi}{2} - \frac{z_1 - z_0}{\Gamma}\right), & z_1 < z_0 < z_2 \\ \Gamma h\left(\frac{\pi}{2} + \frac{z_2 - z_1}{\Gamma} + \arctan\left(\frac{z_0 - z_2}{\Gamma}\right)\right), & z_0 > z_2 \end{cases}$$
$$h = (z_2 - z_1 + \Gamma\pi)^{-1}$$
$$z_0 = \log_{10} t,\ z_1 = \log_{10}(\tau_{\min}),\ z_2 = \log_{10}(\tau_{\max}), \quad (3)$$

where Γ is a control parameter; τ_{min} and τ_{max} stand for the lower and upper limits of the waiting time spectrum. The function $p(t)$ is flat for $z_1 < z < z_2$ and decays as $1/z^2$ outside this range. The decaying rate is controlled by Γ. We fix $\Gamma = 0.8$ in our fitting and use z_1 and z_2 as the field-dependent fitting parameters. The fitted solid curves are presented in Fig. 3. It is clearly shown that the observed polarization switching kinetics can be quite reasonably described by the NLS model.

It is well known that time $\tau_{\max}$ for domain nucleation in the NLS model is determined by the activation field (E_0) for the nucleation in one region, and the time required for these nucleus to expand through the entire region is negligible compared to the waiting time for nucleation.[24] Therefore, $\tau_{\max}$ is considered as the time needed for completely switching each region. Along this line, times $\tau_{\max}$ and $\tau_{\min}$ are used to fit the P_{nz} as a function of t. The values of $\tau_{\max}$ and $\tau_{\min}$ obtained from the fitted curves are plotted in Fig. 4 as a function of field E. Obviously, time $\tau_{\max}$ decreases rapidly with increasing E in an exponential form, indeed indicating the nucleation-dominant polarization switching kinetics, similar to conventional FE systems[25]

$$\tau_{\max} = \frac{\tau_0}{e} \exp(E_0/E)^n, \quad (4)$$

where E_0 is the activated field for polarization switching and τ_0 is the switching time at $E = E_0$, corresponding to the shortest time needed for such nucleation-dominant switching. Usually, an implication of Eq. (4) to a FE system only fits to the case of field E larger than the coercive field, i.e., E_F here ($E_0 > E_F$). However, no convincing fitting of the $\tau_{\max}(E)$ and $\tau_{\min}(E)$ data is possible whatever τ_0 and E_0 are chosen. One example is the curve C(I) shown in the inset of Fig. 4, where $E_0 = 770\,\text{kV/cm}$ and $\tau_0 \sim 10^{-13}\,\text{s}$, as taken from Ref. 25 for $Pb(Zr,Ti)O_3$ thin films. One finds that this curve deviates seriously from the evaluated data (blue solid dots) from the present experiments.

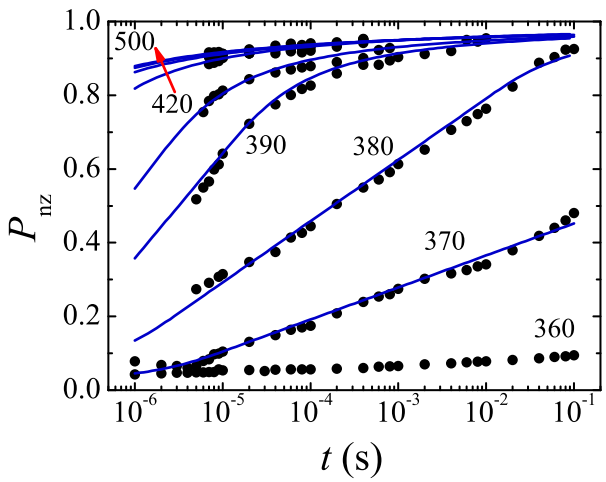

FIG. 3. Time dependent normalized switching polarization (P_{nz}) under various electric fields and room temperature. The unit for the numbers is kV/cm. The symbols denote the PUND measured data and the lines denote the fitting results using the NLS model.

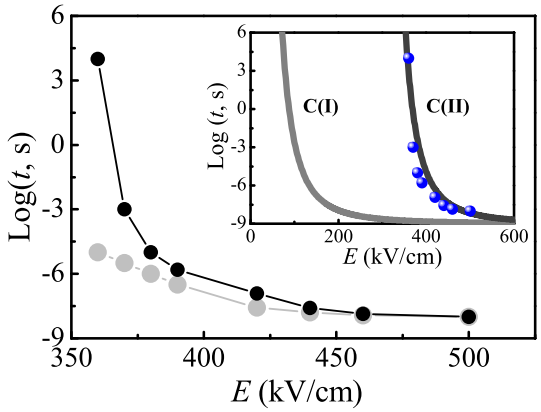

FIG. 4. Maximum waiting time τ_{max} (black dot-lines) and minimum waiting time τ_{min} (gray dot-lines) as functions of electric field E. The solid lines in the inset show the fitting of the experimental data (dots) using Eq. (4) for C(I) and Eq. (5) for C(II) for τ_{max}(E).

One may argue that the failure to fit the measured data on the present AFE films comes from the nature of AFE state. In the other words, the *P-E* hysteresis (double-loop) for an AFE system is phenomenologically equivalent to an imposition of two FE hysteresis loops. Strating from this hypothesis, we can partition the double-loop hysteresis into two single-loops, simply by shifing the central eletric field to $(E_F + E_B)/2$ from the zero point (Here, E_B is the field-induced backward FE → AFE switching field). Thus, Eq. (4) can be re-written by introducing two reduced fields $E' = E - (E_F + E_B)/2$ and $E'_0 = E_0 - (E_F + E_B)/2$, leading to the following equation:

$$\tau_{max} = \frac{\tau_0}{e} \exp\left(E'_0/E'\right)^n. \quad (5)$$

Subsequently, we adopt Eq. (5) to fit the evalutaed data again. It is shown that a quite good fitting can be reached, and the fitted curve C(II) is plotted also in the inset of Fig. 4. Following earlier works[25,26] and our data, we take $n = 2.5$, $E_B = 220$ kV/cm, and $E_F = 380$ kV/cm. The best fitting evaluates a value of $E_0 \sim 455$ kV/cm, consistent with the reported values ($E_F \in$ (300 kV/cm, 550 kV/cm)) for other PLZT-based AFE films.[16,19] Particularly, the extracted τ_0 is as short as 3.0 ns, in good agreement with the values (~10 ns) reported in AFE Pb(Zr, Sn, Ti)O_3 thin films.[27,28]

It is noted that the derived switching time τ_0 in our AFE PLZT films is a bit longer than that for traditional ferroelectrics.[25] One possibility is the difference in the driving field between AFE and ferroelectric systems. The coupling of opposition domains in our AFE PLZT films is omitted in the present work. Such a relaxation of nucleation sites will result in an increase in the switching time. However, the consistency of the experiment results with the prediction of the NLS model modified for our PLZT films suggests that the kinetics of polarization switching in these AFE systems is also governed by the statistics of nucleation. Therefore, the $P(t)$ studies can be used to investigate some issues concerning nonlinear systems, such as E_F/E_B transition and stability of *P-E* loops (or energy storage properties). Moreover, the thermally activated domain-switching kinetics can be viewed as the well-known problem that treats the propagation of nucleus driven by an external field in the presence of a thermally induced bias field.[24] Thus, the ultrafast polarization swithing in our AFE PLZT films is the main reason for the high discharging speed and high stability against varying *f* and *T*, indicating a great promise for pulsed energy storage capacitors.

In summary, we have prepared antiferroelectric $Pb_{0.97}La_{0.02}(Zr_{0.95}Ti_{0.05})O_3$ films with a thickness of 1.2 μm deposited on platinized silicon by chemical solution deposition. The X-ray diffraction and scanning electron microscopy revealed that the PLZT films have highly (001)-preferred orientation with dense and crack-free surfaces and columnar cross-sectional structures. The films could bear a higher energy storage performance (W_{re} of 26.8 J/cm^3 at 1.85 MV/cm and η of 62.5%) with good temperature stability from 25 °C to 270 °C and good frequency stability from 20 Hz to 10 kHz. Finally, the domain kinetics of the AFE films has been discussed within the framework of the NLS theory, implying an ultrafast domain switching time of ~3 ns. Our results suggest that the PLZT 2/95/5 thick films are promising candidates for the high-speed and high-temperature energy density capacitors.

This work was supported by the National 973 Projects of China (2015CB654602) and the National Science Foundation of China (Grant Nos. 51332007, 11574091, and 51272078), the Science and Technology Planning Project of Guangdong Province (Grant No. 2015B090927006), and the Program for International Innovation Cooperation Platform of Guangzhou (No. 2014J4500016).

[1]X. H. Hao, J. W. Zhai, L. B. Kong, and Z. K. Xu, Prog. Mater. Sci. **63**, 1 (2014).
[2]J. Yan, Q. Wang, T. Wei, and Z. J. Fan, Adv. Energy Mater. **4**, 1300816 (2014).
[3]Q. Li, K. Han, M. R. Gadinski, G. Z. Zhang, and Q. Wang, Adv. Mater. **26**, 6244 (2014).
[4]S. Tong, B. H. Ma, M. Narayanan, S. S. Liu, R. Koritala, U. Balachandran, and D. L. Shi, ACS Appl. Mater. Interfaces **5**, 1474 (2013).
[5]B. J. Chu, X. Zhou, K. L. Ren, B. Neese, M. R. Lin, Q. Wang, F. Bauer, and Q. M. Zhang, Science **313**, 334 (2006).
[6]P. Khanchaitit, K. Han, M. R. Gadinski, Q. Li, and Q. Wang, Nat. Commun. **4**, 2845 (2013).
[7]B. H. Ma, Z. Q. Hu, R. E. Koritala, T. H. Lee, S. E. Dorris, and U. Balachandran, J. Mater. Sci.: Mater. Electron. **26**, 9279 (2015).
[8]S. Patel, A. Chauhan, and R. Vaish, Mater. Res. Express **1**, 045502 (2014).
[9]L. Zhang, S. L. Jiang, B. Y. Fan, and G. Z. Zhang, J. Alloys Compd. **622**, 162 (2015).
[10]G. Z. Zhang, D. Y. Zhu, X. S. Zhang, L. Zhang, J. Q. Yi, B. Xie, Y. K. Zeng, Q. Li, Q. Wang, and S. L. Jiang, J. Am. Ceram. Soc. **98**, 1175 (2015).
[11]J. Parui and S. B. Krupanidhi, Appl. Phys. Lett. **92**, 192901 (2008).
[12]Z. Q. Hu, B. H. Ma, S. S. Liu, M. Narayanan, and U. Balachandran, Ceram. Int. **40**, 557 (2014).
[13]J. Ge, X. L. Dong, Y. Chen, F. Cao, and G. S. Wang, Appl. Phys. Lett. **102**, 142905 (2013).
[14]Z. Q. Hu, B. H. Ma, R. E. Koritala, and U. Balachandran, Appl. Phys. Lett. **104**, 263902 (2014).
[15]K. Yao, S. Chen, M. Rahimabady, M. S. Mirshekarloo, S. H. Yu, F. E. H. Tay, T. Sritharan, and L. Lu, IEEE Trans. Ultrason., Ferroelectr., Freq. Control **58**, 1968 (2011).
[16]X. H. Hao, Z. X. Yue, J. B. Xu, S. L. An, and C.-W. Nan, J. Appl. Phys. **110**, 064109 (2011).
[17]Y. Wang, X. H. Hao, J. C. Yang, J. B. Xu, and D. Y. Zhao, J. Appl. Phys. **112**, 034105 (2012).
[18]B. H. Ma, Z. Q. Hu, S. S. Liu, S. Tong, M. Narayanan, R. E. Koritala, and U. Balachandran, Appl. Phys. Lett. **102**, 202901 (2013).

[19]Z. Liu, X. F. Chen, W. Peng, C. H. Xu, X. L. Dong, F. Cao, and G. S. Wang, Appl. Phys. Lett. **106**, 262901 (2015).
[20]Y. Zhao, X. H. Hao, and Q. Zhang, ACS Appl. Mater. Interfaces **6**, 11633 (2014).
[21]X. F. Chen, F. Cao, H. L. Zhang, G. Yu, G. S. Wang, X. L. Dong, Y. Gu, H. L. He, and Y. S. Liu, J. Am. Ceram. Soc. **95**, 1163 (2012).
[22]X. G. Fang, S. X. Lin, A. H. Zhang, X. B. Lu, X. S. Gao, M. Zeng, and J.-M. Liu, Solid State Commun. **219**, 39 (2015).
[23]D. Mao, I. Mejia, H. Stiegler, B. E. Gnade, and M. A. Quevedo-Lopez, J. Appl. Phys. **108**, 094102 (2010).
[24]J. Y. Jo, H. S. Han, J. G. Yoon, T. K. Song, S. H. Kim, and T. W. Noh, Phys. Rev. Lett. **99**, 267602 (2007).
[25]A. K. Tagantsev, I. Stolichnov, N. Setter, J. S. Cross, and M. Tsukada, Phys. Rev. B **66**, 214109 (2002).
[26]Y. W. So, D. J. Kim, T. W. Noh, J.-G. Yoon, and T. K. Song, Appl. Phys. Lett. **86**, 092905 (2005).
[27]B. M. Xu, P. Moses, N. G. Pai, and L. E. Cross, Appl. Phys. Lett. **72**, 593 (1998).
[28]C. W. Ahn, G. Amarsanaa, S. S. Won, S. A. Chae, D. S. Lee, and I. W. Kim, ACS Appl. Mater. Interfaces **7**, 26381 (2015).
[29]See supplementary material at http://dx.doi.org/10.1063/1.4944645 for details of the solution preparation and deposition conditions, XRD pattern, planar and cross-sectional SEM images, *P-E* loops at various electric fields, and a schematic of the PUND measurement.